

Sharp bounds of constants in Poincaré type inequalities for polygonal domains

S. Matculevich and S. Repin

Department of Mathematical Information Technology, University of Jyväskylä
 FIN-40100 Jyväskylä, FINLAND
 e-mails: svetlana.v.matculevich@jyu.fi, sergey.repin@jyu.fi

St. Petersburg Dept. of V.A. Steklov Institute of Mathematics of RAS
 St. Petersburg, Russia

February 15, 2019

Abstract

The paper is concerned with sharp estimates of constants in Poincaré type inequalities for functions having zero mean value in a simplicial domain or on a part of its boundary. These estimates are important for quantitative analysis of problems generated by differential equations where numerical approximations are typically constructed with the help of simplicial meshes. We suggest easily computable relations that provide sharp bounds of the respective constants and compare these results to analytical estimates (if they are known). In the last section, we present an example that shows possible applications of the results and derive a computable majorant of the difference between the exact solution of a boundary value problem and an arbitrary finite dimensional approximation computed on a simplicial mesh.

1 Introduction

Let Ω be an open bounded connected domain in \mathbb{R}^d ($d \geq 2$) with Lipschitz boundary $\partial\Omega$. It is well known that the Poincaré inequality ([15, 16])

$$\|w\|_{\Omega} \leq C_{\Omega}^{\text{P}} \|\nabla w\|_{\Omega} \quad (1)$$

holds for any

$$w \in \tilde{H}^1(\Omega) := \left\{ w \in H^1(\Omega) \mid \{w\}_{\Omega} = 0 \right\},$$

where $\|w\|_{\Omega}$ denotes the norm in $L^2(\Omega)$, $\{w\}_{\Omega} := \frac{1}{|\Omega|} \int_{\Omega} w \, dx$ is the mean value of w , and $|\Omega|$ is the Lebesgue measure of Ω . The constant C_{Ω} depends only on Ω and d .

Poincaré type inequalities also hold for

$$w \in \tilde{H}^1(\Omega, \Gamma) := \left\{ w \in H^1(\Omega) \mid \{w\}_{\Gamma} = 0 \right\},$$

where Γ is a measurable part of $\partial\Omega$ such that $\text{meas}_{d-1}\Gamma > 0$ (in particular, Γ may coincide with the whole boundary). For any $w \in \tilde{H}^1(\Omega, \Gamma)$, we have two inequalities similar to (1). The first one

$$\|w\|_{\Omega} \leq C_{\Gamma}^{\text{P}} \|\nabla w\|_{\Omega} \quad (2)$$

is another form of the Poincaré inequality (1), which is stated for a different set of functions and contains a different constant. The constant C_{Γ}^{P} is associated with the minimal positive eigenvalue of the problem

$$-\Delta u = \lambda u \text{ in } T; \quad \partial_n u = \lambda \{u\} \text{ on } \Gamma; \quad \partial_n u = 0 \text{ on } \partial T \setminus \Gamma, \quad \forall u \in H^1(\Omega, \Gamma). \quad (3)$$

The second inequality

$$\|w\|_{\Gamma} \leq C_{\Gamma}^{\text{Tr}} \|\nabla w\|_{\Omega} \quad (4)$$

estimates the trace of $w \in \tilde{H}^1(\Omega, \Gamma)$ on Γ . It is associated with the minimal non-zero eigenvalue of the problem

$$-\Delta u = 0 \text{ in } T; \quad \partial_n u = \lambda u \text{ on } \Gamma; \quad \partial_n u = 0 \text{ on } \partial T \setminus \Gamma, \quad \forall u \in H^1(\Omega, \Gamma). \quad (5)$$

Poincaré type inequalities are often used in analysis of nonconforming approximations (e.g., discontinuous Galerkin or mortar methods), domain decomposition methods (see, e.g., [7, 5] and [19]), analysis of problems described in terms of vector valued functions (see, e.g., [6, 13]), a posteriori estimates, and other applications related to quantitative analysis of partial differential equations.

Therefore, exact values of respective constants (or sharp and guaranteed bounds of them) are interesting from both analytical and computational points of view.

It is known that for convex domains $C_\Omega^P \leq \frac{\text{diam}(\Omega)}{\pi}$ (see [14]). For isosceles triangles, this estimate was improved in [8], where it was shown that

$$C_\Omega^P \leq \overline{C}_T^{LS} := \text{diam}\Omega \cdot \begin{cases} \frac{1}{j_{1,1}} & \alpha \in (0, \frac{\pi}{3}], \\ \min \left\{ \frac{1}{j_{1,1}}, \frac{1}{j_{0,1}} (2(\pi - \alpha) \tan(\alpha/2))^{-1/2} \right\} & \alpha \in (\frac{\pi}{3}, \frac{\pi}{2}], \\ \frac{1}{j_{0,1}} (2(\pi - \alpha) \tan(\alpha/2))^{-1/2} & \alpha \in (\frac{\pi}{2}, \pi]. \end{cases} \quad (6)$$

Here, $j_{0,1} \approx 2.4048$ and $j_{1,1} \approx 3.8317$ are the smallest positive roots of the Bessel functions J_0 and J_1 , respectively. A lower bound of C_Ω for convex domains was derived in [3]. It was shown that

$$C_\Omega^P \geq \frac{\text{diam}\Omega}{2j_{0,1}}. \quad (7)$$

This estimate compliments the upper bound presented by the Payne–Weinberger estimate. According to [1], the estimate (7) is known to be the best lower bound among all known so far. Exact values of C_Γ^P and C_Γ^{Tr} were derived in [12] for parallelepipeds, rectangles, and right triangles. Below, we present a concise summary of these results related to the case $d = 2$:

1. If $T := \text{conv}\{(0, 0), (0, h), (h, 0)\}$, and $\Gamma := \{x_1 = 0, x_2 \in [0, h]\}$ (i.e., Γ coincides with one of the legs of the isosceles right triangle), then

$$C_\Gamma^P = \frac{h}{\zeta_0}, \quad \text{and} \quad C_\Gamma^{\text{Tr}} = \left(\frac{h}{\zeta_0 \tanh(\hat{\zeta}_0)} \right)^{1/2}, \quad (8)$$

where ζ_0 and $\hat{\zeta}_0$ are unique roots in $(0, \pi)$ of the equations

$$z \cot(z) + 1 = 0 \quad \text{and} \quad \tan(z) + \tanh(z) = 0, \quad (9)$$

respectively.

2. If $T := \text{conv}\{(0, 0), (0, h), (\frac{h}{2}, \frac{h}{2})\}$ and Γ coincides with the hypotenuse of the isosceles right triangle, then

$$C_\Gamma^P = \frac{h}{2\zeta_0}, \quad \text{and} \quad C_\Gamma^{\text{Tr}} = \left(\frac{h}{2} \right)^{1/2}.$$

Above mentioned results form a basis for getting sharp bounds of the constants C_Γ^P and C_Γ^{Tr} , and C_Ω^P for arbitrary non-degenerate triangles and tetrahedrons, which are typical objects in various discretization methods. In Section 2, we deduce guaranteed and easily computable bounds of C_Γ^P and C_Γ^{Tr} for arbitrary non-degenerate triangles. The efficiency of these bounds is tested in Section 3, where they are compared with lower bounds computed numerically by minimization of the respective quotients over sufficiently representative sets of trial functions. In the same section, we make a similar comparison of numerical lower bounds related to the constant C_Ω^P with upper and lower estimates studied in [14, 8] and [3]. Section 4 is devoted to tetrahedrons. We combine numerical and theoretical estimates in order to derive two sided bounds of the constants. Finally, in Section 5 we present an example that shows one possible application of the estimates considered in previous sections. Here, the constants are used in order to deduce a guaranteed and fully computable upper bound of the distance between the exact solution of an elliptic boundary value problem and an arbitrary function (approximation) in the respective energy space.

2 Majorants of C_Γ^P and C_Γ^{Tr} for triangular domains

We set

$$T = \text{conv}\{(0, 0), (h, 0), (h\rho \cos \alpha, h\rho \sin \alpha)\} \quad \text{and} \quad \Gamma := \{x_1 \in [0, h]; x_2 = 0\},$$

where $\rho > 0$, $h > 0$, and $\alpha \in (0, \pi)$ are geometrical parameters that fully define a triangle T (see Fig. 1). Easily computable bounds of C_Γ^P and C_Γ^{Tr} are presented below.

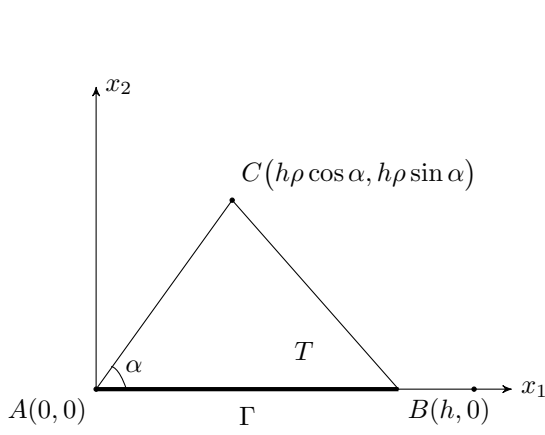


Figure 1: Simplex in \mathbb{R}^2 .

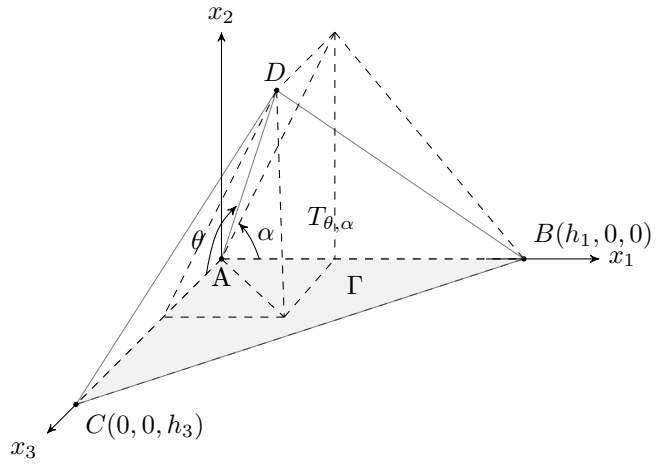


Figure 2: Simplex in \mathbb{R}^3 .

Lemma 1 For any $w \in \tilde{H}^1(T, \Gamma)$, the estimates

$$\|w\|_T \leq C_\Gamma^P h \|\nabla w\|_T \quad \text{and} \quad \|w\|_\Gamma \leq C_\Gamma^{\text{Tr}} h^{1/2} \|\nabla w\|_T \quad (10)$$

hold with

$$\overline{C}_\Gamma^P = \min \left\{ c_{\pi/2}^P C_{\hat{\Gamma}, \pi/2}^P, c_{\pi/4}^P C_{\hat{\Gamma}, \pi/4}^P \right\} \quad \text{and} \quad \overline{C}_\Gamma^{\text{Tr}} = \min \left\{ c_{\pi/2}^{\text{Tr}} C_{\hat{\Gamma}, \pi/2}^{\text{Tr}}, c_{\pi/4}^{\text{Tr}} C_{\hat{\Gamma}, \pi/4}^{\text{Tr}} \right\},$$

respectively. Here,

$$c_{\pi/2}^P = \mu_{\pi/2}^{1/2}, \quad c_{\pi/2}^{\text{Tr}} = (\rho \sin \alpha)^{-1/2} c_{\pi/2}^P, \quad c_{\pi/4}^P = \mu_{\pi/4}^{1/2}, \quad c_{\pi/4}^{\text{Tr}} = (2\rho \sin \alpha)^{-1/2} c_{\pi/4}^P,$$

where

$$\mu_{\pi/2}(\rho, \alpha) = \frac{1}{2} \left(1 + \rho^2 + (1 + \rho^4 + 2\rho^2 \cos 2\alpha)^{1/2} \right), \quad (11)$$

$$\mu_{\pi/4}(\rho, \alpha) = 2\rho^2 - 2\rho \cos \alpha + 1 + ((2\rho^2 + 1)(2\rho^2 + 1 - 4\rho \cos \alpha + 4\rho^2 \cos 2\alpha))^{1/2}, \quad (12)$$

and $C_{\hat{\Gamma}, \pi/2}^P \approx 0.49291$, $C_{\hat{\Gamma}, \pi/2}^{\text{Tr}} \approx 0.65602$ and $C_{\hat{\Gamma}, \pi/4}^P \approx 0.24646$, $C_{\hat{\Gamma}, \pi/4}^{\text{Tr}} \approx 0.70711$.

Proof: Consider a linear mapping $\mathcal{F}_{\pi/2} : \hat{T}_{\pi/2} \rightarrow T$

$$x = \mathcal{F}_{\pi/2}(\hat{x}) = B_{\pi/2} \hat{x}, \quad \text{where} \quad B_{\pi/2} = \begin{pmatrix} h & \rho h \cos \alpha \\ 0 & \rho h \sin \alpha \end{pmatrix}, \quad \det B_{\pi/2} = \rho h^2 \sin \alpha.$$

For any $\hat{w} \in \tilde{H}^1(\hat{T}_{\pi/2}, \hat{\Gamma})$, we have the estimate

$$\|\hat{w}\|_{\hat{T}_{\pi/2}} \leq C_{\hat{\Gamma}, \pi/2}^P \|\nabla \hat{w}\|_{\hat{T}_{\pi/2}}, \quad (13)$$

where $C_{\hat{\Gamma}, \pi/2}^P$ is the constant associated with the basic simplex $T_{\pi/2} := \text{conv}\{(0,0), (1,0), (0,1)\}$. Note that

$$\|\hat{w}\|_{\hat{T}_{\pi/2}}^2 = \frac{1}{\rho h^2 \sin \alpha} \|w\|_T^2, \quad (14)$$

and

$$\|\nabla \hat{w}\|_{\hat{T}_{\pi/2}}^2 \leq \frac{1}{\rho h^2 \sin \alpha} \int_T A_{\pi/2}(h, \rho, \alpha) \nabla w \cdot \nabla w \, dx,$$

where

$$A_{\pi/2}(h, \rho, \alpha) = h^2 \begin{pmatrix} 1 + \rho^2 \cos^2 \alpha & \rho^2 \sin \alpha \cos \alpha \\ \rho^2 \sin \alpha \cos \alpha & \rho^2 \sin^2 \alpha \end{pmatrix}.$$

It is not difficult to see that

$$\lambda_{\max}(A_{\frac{\pi}{2}}) = h^2 \mu_{\pi/2}(\rho, \alpha), \quad \mu_{\pi/2}(\rho, \alpha) = \frac{1}{2} \left(1 + \rho^2 + (1 + \rho^4 + 2 \cos 2\alpha \rho^2)^{1/2} \right),$$

where $\mu_{\pi/2}(\rho, \alpha)$ is defined in (11). We use (13), (14), and (??), and obtain

$$\|w\|_T \leq c_{\pi/2}^{\text{P}} C_{\widehat{\Gamma}, \pi/2}^{\text{P}} h \|\nabla w\|_T, \quad c_{\pi/2}^{\text{P}}(\rho, \alpha) = \mu_{\pi/2}^{1/2}(\rho, \alpha). \quad (15)$$

Next, in view of (4), for any $\hat{w} \in \widetilde{H}^1(\widehat{T}_{\pi/2}, \widehat{\Gamma})$ we have

$$\|\hat{w}\|_{\widehat{\Gamma}} \leq C_{\widehat{\Gamma}, \pi/2}^{\text{Tr}} \|\nabla \hat{w}\|_{\widehat{T}_{\pi/2}},$$

where $C_{\widehat{\Gamma}, \pi/2}^{\text{Tr}}$ is the constant associated with the reference simplex $\widehat{T}_{\pi/4} := \text{conv}\left\{(0, 0), (1, 0), \left(\frac{1}{2}, \frac{1}{2}\right)\right\}$. Since

$$\|\hat{w}\|_{\widehat{\Gamma}}^2 = \frac{1}{h} \|w\|_{\Gamma}^2,$$

we obtain

$$\|w\|_{\Gamma} \leq c_{\pi/2}^{\text{Tr}} C_{\widehat{\Gamma}, \pi/2}^{\text{Tr}} h^{1/2} \|\nabla w\|_T, \quad c_{\pi/2}^{\text{Tr}}(\rho, \alpha) = \left(\frac{\mu_{\pi/2}(\rho, \alpha)}{\rho \sin \alpha}\right)^{1/2}. \quad (16)$$

The mapping

$$x = \mathcal{F}_{\pi/4}(\hat{x}) = B_{\pi/4} \hat{x}, \quad \text{where } B_{\Pi} = \begin{pmatrix} h & 2\rho h \cos \alpha - h \\ 0 & 2\rho h \sin \alpha \end{pmatrix} \quad \text{and} \quad \det B_{\pi/4} = 2\rho h^2 \sin \alpha > 0,$$

yields another pair of estimates for the functions in $\widetilde{H}^1(T, \Gamma)$:

$$\|w\|_T \leq c_{\pi/4}^{\text{P}} C_{\widehat{\Gamma}, \pi/4}^{\text{P}} h \|\nabla w\|_T, \quad c_{\pi/4}^{\text{P}}(\rho, \alpha) = \mu_{\pi/4}^{1/2}(\rho, \alpha), \quad (17)$$

and

$$\|w\|_{\Gamma} \leq c_{\pi/4}^{\text{Tr}} C_{\widehat{\Gamma}, \pi/4}^{\text{Tr}} h^{1/2} \|\nabla w\|_T, \quad c_{\pi/4}^{\text{Tr}}(\rho, \alpha) = \left(\frac{\mu_{\pi/4}(\rho, \alpha)}{2\rho \sin \alpha}\right)^{1/2}, \quad (18)$$

where $\mu_{\pi/4}(\rho, \alpha)$ is defined in (12). Now, (10) follows from (15), (16), (17), and (18). \square

3 Minorants of C_{Γ}^{P} and C_{Γ}^{Tr} for triangular domains

3.1 Two-sided bounds of C_{Γ}^{P} and C_{Γ}^{Tr}

Majorants of C_{Γ}^{P} and C_{Γ}^{Tr} provided by Lemma 1 should be compared with the corresponding minorants, which can be found by minimization of the Rayleigh quotients

$$\mathcal{R}_{\Gamma}^{\text{P}}[w] = \frac{\|\nabla w\|_T}{\|w - \{w\}_{\Gamma}\|_T} \quad \text{and} \quad \mathcal{R}_{\Gamma}^{\text{Tr}}[w] = \frac{\|\nabla w\|_T}{\|w - \{w\}_{\Gamma}\|_{\Gamma}},$$

over finite dimensional subspaces $V^N \subset H^1(T)$ formed with by sufficiently representative collections of test functions. For this purpose, we use either power or Fourier series and introduce the respective subspaces

$$V_1^N := \text{span}\left\{x^i y^j\right\}, \quad \text{and} \quad V_2^N := \text{span}\left\{\cos(\pi i x) \cos(\pi j y)\right\}, \quad i, j = 0, \dots, N, \quad i = j \neq 0.$$

Note that $\dim V_1^N = \dim V_2^N = M(N) := (N+1)^2 - 1$. The corresponding constants are denoted by $\underline{C}_{\Gamma}^{M, \text{P}}$ and $\underline{C}_{\Gamma}^{M, \text{Tr}}$.

The spaces V_1^N and V_2^N are also used for analysis of the quotient $\mathcal{R}_T[w] = \frac{\|\nabla w\|_T}{\|w - \{w\}_T\|_T}$, which yields lower bounds of the constant in (1) denoted by $\underline{C}_T^{M, \text{P}}$. Since above defined finite dimensional spaces are limit dense in H^1 , the minorants tend to exact constants as $M(N)$ tends to infinity. Table 1 demonstrates that the ratios between exact constants and their approximate values are quite close to 1 even for relatively small N . In tests discussed below, we select $N = 6$ or 7 .

In Figs 3a and 3c, we depict $\underline{C}_{\Gamma}^{M, \text{P}}$ for $M(N) = 48$ (thin line) for different T with $\rho = \frac{\sqrt{2}}{2}$, $\rho = 1$, and different $\alpha \in (0, \pi)$. Guaranteed upper bounds $\overline{C}_{\pi/2}^{\text{P}} = c_{\pi/2}^{\text{P}} C_{\widehat{\Gamma}, \pi/2}^{\text{P}}$ and $\overline{C}_{\pi/4}^{\text{P}} = c_{\pi/4}^{\text{P}} C_{\widehat{\Gamma}, \pi/4}^{\text{P}}$ are depicted by dashed lines. By the bold line, we emphasize of $\overline{C}_{\pi/2}^{\text{P}}$ and $\overline{C}_{\pi/4}^{\text{P}}$, which presents $\overline{C}_{\Gamma}^{\text{P}}$ as it is defined in Lemma 1. Analogously in Figs 4a

		$\alpha = \frac{\pi}{2}, \rho = 1$		$\alpha = \frac{\pi}{4}, \rho = \frac{\sqrt{2}}{2}$	
N	$M(N)$	$\underline{c}_{\mathbf{p}, \pi/2}^M$	$\underline{c}_{\text{Tr}, \pi/2}^M$	$\underline{c}_{\mathbf{p}, \pi/4}^M$	$\underline{c}_{\text{Tr}, \pi/4}^M$
1	3	0.8801	0.9561	0.8647	1.0000
2	8	0.9945	0.9898	0.9925	1.0000
3	15	0.9999	0.9998	0.9962	1.0000
4	24	1.0000	0.9999	1.0000	1.0000
5	35	1.0000	1.0000	1.0000	1.0000
6	48	1.0000	1.0000	1.0000	1.0000

Table 1: Ratios of $\underline{c}_{\mathbf{p}, \pi/2}^M$, $\underline{c}_{\text{Tr}, \pi/2}^M$ and $\underline{c}_{\mathbf{p}, \pi/4}^M$, $\underline{c}_{\text{Tr}, \pi/4}^M$ with respect to increasing N and $M(N)$.

		$\rho = \frac{\sqrt{2}}{2}$				$\rho = 1$			
α		$\underline{C}_{\Gamma}^{48, \mathbf{p}}$	$\overline{C}_{\Gamma}^{\mathbf{p}}$	$\underline{C}_{\Gamma}^{48, \text{Tr}}$	$\overline{C}_{\Gamma}^{\text{Tr}}$	$\underline{C}_{\Gamma}^{48, \mathbf{p}}$	$\overline{C}_{\Gamma}^{\mathbf{p}}$	$\underline{C}_{\Gamma}^{48, \text{Tr}}$	$\overline{C}_{\Gamma}^{\text{Tr}}$
$\pi/18$		0.2429	0.2657	1.2786	1.5386	0.3245	0.3486	1.2572	1.6971
$\pi/9$		0.2414	0.2627	0.9289	1.0838	0.3248	0.3493	0.9058	1.2116
$\pi/6$		0.2389	0.2577	0.7919	0.8792	0.3268	0.3527	0.7632	1.0118
$2\pi/9$		0.2379	0.2507	0.7259	0.7543	0.3339	0.3636	0.6906	0.9201
$5\pi/18$		0.2632	0.2722	0.6945	0.7503	0.3514	0.3884	0.6529	0.9003
$\pi/3$		0.3008	0.3220	0.6829	0.8348	0.3809	0.4269	0.6362	0.8634
$7\pi/18$		0.3382	0.3694	0.6840	0.8432	0.4173	0.4721	0.6332	0.7840
$4\pi/9$		0.3740	0.4140	0.6947	0.7973	0.4556	0.5187	0.6404	0.7162
$\pi/2$		0.4075	0.4554	0.7136	0.7801	0.4929	0.4929	0.6560	0.6560
$5\pi/9$		0.4382	0.4933	0.7409	0.7973	0.5280	0.5340	0.6797	0.7162
$11\pi/18$		0.4660	0.5165	0.7779	0.8432	0.5600	0.5710	0.7125	0.7840
$2\pi/3$		0.4905	0.5361	0.8274	0.9118	0.5884	0.6037	0.7569	0.8634
$13\pi/18$		0.5115	0.5552	0.8948	1.0040	0.6129	0.6318	0.8175	0.9607
$7\pi/9$		0.5289	0.5720	0.9898	1.1292	0.6332	0.6550	0.9033	1.0874
$5\pi/6$		0.5426	0.5856	1.1334	1.3107	0.6492	0.6733	1.0332	1.2673
$8\pi/9$		0.5524	0.5956	1.3796	1.6118	0.6607	0.6865	1.2565	1.5623
$17\pi/18$		0.5583	0.6017	1.9436	2.2851	0.6676	0.6944	1.7692	2.2179

Table 2: Lower and upper bounds of $C_{\Gamma}^{\mathbf{p}}$ and C_{Γ}^{Tr} with respect to α and for $\rho = \frac{\sqrt{2}}{2}$ and 1.

and 4b, the lower bound $\underline{C}_{\Gamma}^{M, \text{Tr}}$ (for $M(N) = 48$) of the constant C_{Γ}^{Tr} is presented together with the upper bound $\overline{C}_{\Gamma}^{\text{Tr}}$ (which is defined as minimum of $\overline{C}_{\pi/2}^{\text{Tr}} = c_{\pi/2}^{\text{Tr}} C_{\widehat{\Gamma}, \pi/2}^{\text{Tr}}$ and $\overline{C}_{\pi/4}^{\text{Tr}} = c_{\pi/4}^{\text{Tr}} C_{\widehat{\Gamma}, \pi/4}^{\text{Tr}}$; dashed lines. In the digital form, the information is represented in Table 2.

Fig 3a corresponds to the case $\rho = \frac{\sqrt{2}}{2}$. It is worth noting that for $\alpha = \frac{\pi}{4}$ the lower bound $\underline{C}_{\Gamma}^{M, \mathbf{p}}$ coincides with constant $C_{\Gamma}^{\mathbf{p}}$ ($\overline{C}_{\pi/4}^{\mathbf{p}}$). This happens because for $\alpha = \frac{\pi}{4}$ the mapping $\mathcal{F}_{\pi/4}$ is identical (see, e.g., Fig 3b). Analogous coincidence can be observed for C_{Γ}^{Tr} ($\overline{C}_{\pi/4}^{\text{Tr}}$) in Fig 4a. In Fig 3c, the curve corresponding to $\underline{C}_{\Gamma}^{M, \mathbf{p}}$ coincides with the line of $C_{\Gamma}^{\mathbf{p}}$ ($\overline{C}_{\pi/2}^{\mathbf{p}}$) at the point $\alpha = \frac{\pi}{2}$ (due to the fact for this angle \mathcal{F} is the identical mapping and T coincides with $\widehat{T}_{\pi/2}$ (see Fig 3d). Fig 4b exposes similar results for $\underline{C}_{\Gamma}^{M, \text{Tr}}$ and C_{Γ}^{Tr} ($\overline{C}_{\pi/2}^{\text{Tr}}$).

3.2 Two-sided bounds of $C_{\Gamma}^{\mathbf{p}}$ and C_{Γ}^{Tr}

Above discussed method can be used, if we wish to obtain two-sided bounds of the constant in (1) for an arbitrary triangle T . Minimization of $\mathcal{R}[w] = \frac{\|\nabla w\|_T}{\|w - \{w\}_T\|_T}$ over $V_1^N \subset H^1(T)$ yields a guaranteed lower bound $\underline{C}_T^{M, \mathbf{p}}$. The values computed by this procedure are compared with $\overline{C}_T^{\mathbf{p}} := \frac{\text{diam} T}{\pi}$ and $\underline{C}_T^{\mathbf{p}} := \frac{\text{diam} T}{2j_{0,1}}$ (see (??)). In Fig 5, we compare $\underline{C}_T^{M, \mathbf{p}}$ ($M(N) = 48$) with $\overline{C}_T^{\mathbf{p}}$ and $\underline{C}_T^{\mathbf{p}}$ for T with $\rho = \frac{\sqrt{2}}{2}, 1$, and $\frac{3}{2}$. We see that \underline{C}_T^{48} indeed lies within the admissible two-sided bound. True values of the constant lie between the bold and dashed lines, but closer to the bold line, which practically illustrate the constant (this follows from the fact that $M(N)$ does not noticeable change the line, e.g., for $\rho = 1$ and $M(N) = 63$ maximal difference with respect to Fig. does not exceed $1e - 8$). Also, we note that, the lower bound $\underline{C}_T^{\mathbf{p}}$ is much sharper, and, moreover, asymptotically exact for $\alpha \rightarrow \pi$. Due to [8], we know the improved upper bound \overline{C}_T^{LS} for isosceles triangles (see 6). In Fig 6, it is easy to see that \overline{C}_T^{LS} is rather accurate and for $\alpha \rightarrow 0$ and $\alpha \rightarrow \pi$ provide almost exact estimates. Moreover, the lower bound \underline{C}_T^{48} indeed converges to $\frac{\text{diam} T}{j_{1,1}}$ as T degenerates when α tends to 0 (see [8]).

3.3 Shape of the minimizer

Exact constants in (2) and (4) are generated by minimal positive eigenvalues of the eigenvalue problems (3) and (5). In this section, we present results related to the respective eigenfunctions. In order to depict all of them in a unified form, we use the barycentric coordinates $\lambda_i \in (0, 1)$, $i = 1, 2, 3$, $\sum_{i=1}^3 \lambda_i = 1$. Figs 7 and 8 show eigenfunctions computed for isosceles triangles with different angles α between two legs (zero mean condition is imposed on one of the legs). The eigenfunctions were computed in the process of finding $\underline{C}_\Gamma^{M,P}$ and $\underline{C}_\Gamma^{M,Tr}$. All the eigenfunctions are normalized such that the maximal value of a function is equal to 1.

For $\alpha = \frac{\pi}{2}$, the exact eigenfunction associated with the smallest positive eigenvalue $\lambda_\Gamma^P = (\frac{z_0}{h})^2$, is known (see [12]). It is (see Fig 7d)

$$u_\Gamma^P = \cos(\frac{z_0 x_1}{h}) + \cos(\frac{z_0(x_2 - h)}{h}),$$

where z_0 is the root of the first equation in (9). We can compare it with the approximate eigenfunction $u_\Gamma^{M,P}$ computed by minimization of $\mathcal{R}_\Gamma^P[w]$. It is depicted in Fig 7c.

Analogous results for eigenfunctions related to the constant $\underline{C}_\Gamma^{M,Tr}$ are presented in Fig. 8. Again, for $\alpha = \frac{\pi}{2}$ we know the exact eigenfunction exact eigenfunction

$$u_\Gamma^{Tr} = \cos(\hat{z}_0 x_1) \cosh(\hat{z}_0(x_2 - h)) + \cosh(\hat{z}_0 x_1) \cos(\hat{z}_0(x_2 - h)),$$

where \hat{z}_0 is the root of second equation in (9) (see Fig 8d), which minimizes the quotient $\mathcal{R}_\Gamma^{Tr}[w]$ associated with the smallest positive eigenvalue $\lambda_\Gamma^{Tr} = \frac{\hat{z}_0 \tanh(\hat{z}_0)}{h}$. It is easy to see that with the assigned value of $M(N)$ numerical approximation practically coincides with the exact one.

In the above considered examples, the eigenfunctions associated with minimal positive eigenvalues expose a continuous evolution with respect to α . However, this may be not true for the quotient $\mathcal{R}_T[w]$, where the minimizer may cardinally change the profile. Fig 6 indicates a possibility of such rapid change at $\alpha = \frac{\pi}{3}$, where the curve (related to \underline{C}_T^{48}) obviously becomes nonsmooth. This happens because the function, minimizing $\mathcal{R}_T[w]$ over V_1^N , changes qualitatively. Figs 9d–9i show three eigenfunctions $u_{T,1}^{48}$, $u_{T,2}^{48}$, and $u_{T,3}^{48}$ related to three minimal eigenvalues $\lambda_{T,1}^{48}$, $\lambda_{T,2}^{48}$, and $\lambda_{T,3}^{48}$ computed in the process of minimization of $\mathcal{R}_T[w]$. The functions are computed for isosceles triangles and are sorted in accordance with values of the respective eigenvalues. Fig 9 illustrates these three eigenfunctions for T with angles $\alpha = \frac{\pi}{3}$, $\frac{\pi}{3} + \varepsilon$, and $\frac{\pi}{3} - \varepsilon$, $\varepsilon = \frac{\pi}{36}$. It is seen that at $\alpha = \pi/3$ the first and the second eigenfunctions change places. Table 3 presents the corresponding results in the digital form.

It is worth noting that for equilateral triangles two minimal eigenfunctions are known (see [10]):

$$u_1 = \cos\left(\frac{2\pi}{3}(2x_1 - 1)\right) - \cos\left(\frac{2\pi}{\sqrt{3}}x_2\right) \cos\left(\frac{\pi}{3}(2x_1 - 1)\right),$$

$$u_2 = \sin\left(\frac{2\pi}{3}(2x_1 - 1)\right) + \cos\left(\frac{2\pi}{\sqrt{3}}x_2\right) \sin\left(\frac{\pi}{3}(2x_1 - 1)\right).$$

These functions practically coincide with the functions $u_{T,1}^{48}$ and $u_{T,2}^{48}$ presented in Fig 9d. Finally, we note that this phenomenon (change of the minimal eigenfunction) was observed only for isosceles triangles. It did not appear if, e.g., $\rho = \frac{\sqrt{2}}{2}$ or $\rho = \frac{3}{2}$. The eigenvalues as well as the constants corresponding to the eigenfunctions presented in Figs 9 are summarized in the Table 3.

		$\frac{\pi}{3} - \varepsilon$		$\frac{\pi}{3}$		$\frac{\pi}{3} + \varepsilon$	
	$u_{T,i}^M$	$\underline{C}_{T,i}^{48}$	$\lambda_{T,i}^{48}$	$\underline{C}_{T,i}^{48}$	$\lambda_{T,i}^{48}$	$\underline{C}_{T,i}^{48}$	$\lambda_{T,i}^{48}$
$\rho = 1$	$u_{T,1}^{48}$	0.2419	17.0951	0.2387	17.5463	0.2537	15.5404
	$u_{T,2}^{48}$	0.2229	20.1216	0.2387	17.5463	0.2355	18.0309
	$u_{T,3}^{48}$	0.1353	54.6024	0.1378	52.6396	0.1422	49.4818
$\rho = \frac{\sqrt{2}}{2}$	$u_{T,1}^{48}$	0.23137	18.6804	0.23671	17.8471	0.24336	16.8850
	$u_{T,2}^{48}$	0.17082	34.2707	0.17435	32.8970	0.17642	32.1295
	$u_{T,3}^{48}$	0.1229	66.2058	0.12789	61.1402	0.13298	56.5493
$\rho = \frac{3}{2}$	$u_{T,1}^{48}$	0.34714	8.2983	0.35523	7.9247	0.3648	7.5143
	$u_{T,2}^{48}$	0.24485	16.6801	0.24885	16.1482	0.25125	15.8412
	$u_{T,3}^{48}$	0.18258	29.9981	0.19084	27.4575	0.19845	25.3921

Table 3: $\underline{C}_T^{M,P}$ and λ_T^M corresponding to the first three eigenfunctions in Fig. 9.

4 Two-sided bounds of C_{Γ}^{P} and C_{Γ}^{Tr} for tetrahedrons

A nondegenerate tetrahedron $T \in \mathbb{R}^3$ can be presented in the form

$$T = \text{conv}\left\{(0, 0, 0), (h_1, 0, 0), (0, 0, h_3), (D_{x_1}, D_{x_2}, D_{x_3})\right\}, \quad (19)$$

where $(D_{x_1}, D_{x_2}, D_{x_3}) = (h_1 \rho \cos \alpha \sin \theta, h_1 \rho \sin \alpha \sin \theta, h_1 \rho \cos(\theta))$, h_1 and h_3 are the scaling parameters along axes O_{x_1} and O_{x_3} , respectively, α is a polar angle, and θ is an azimuthal angle (see Fig. 2). Let zero mean condition be imposed on

$$\Gamma = \text{conv}\left\{(0, 0, 0), (h_1, 0, 0), (0, 0, h_3)\right\},$$

and $\widehat{T}_{\hat{\theta}, \hat{\alpha}}$ denote the reference tetrahedron, where $\hat{\theta}$ and $\hat{\alpha}$ are fixed angles. Then, by $\mathcal{F}_{\hat{\theta}, \hat{\alpha}}$ we denote the respective mapping $\mathcal{F}_{\hat{\theta}, \hat{\alpha}}: \widehat{T}_{\hat{\theta}, \hat{\alpha}} \rightarrow T$. To the best of our knowledge, exact values of constants in Poincaré type inequalities for simplexes in \mathbb{R}^3 are unknown. Therefore, we first consider several reference tetrahedrons with $\rho = 1$, $\hat{\theta} = \frac{\pi}{2}$, and $\hat{\alpha}_1 = \frac{\pi}{4}$, $\hat{\alpha}_2 = \frac{\pi}{3}$, $\hat{\alpha}_3 = \frac{\pi}{2}$, and $\hat{\alpha}_4 = \frac{2\pi}{3}$, and find the constants numerically with high accuracy. Table 4 shows convergence of the constants with respect to increasing $M(N)$. Then, for an arbitrary tetrahedron T , we have

	$\hat{\theta} = \frac{\pi}{2}, \hat{\alpha} = \frac{\pi}{4}$		$\hat{\theta} = \frac{\pi}{2}, \hat{\alpha} = \frac{\pi}{3}$		$\hat{\theta} = \frac{\pi}{2}, \hat{\alpha} = \frac{\pi}{2}$		$\hat{\theta} = \frac{\pi}{2}, \hat{\alpha} = \frac{2\pi}{3}$	
$M(N)$	$C_{\widehat{\Gamma}, \pi/2, \hat{\alpha}}^{\text{P}, M}$	$C_{\widehat{\Gamma}, \pi/2, \hat{\alpha}}^{\text{Tr}, M}$	$C_{\widehat{\Gamma}, \pi/2, \hat{\alpha}}^{\text{P}, M}$	$C_{\widehat{\Gamma}, \pi/2, \hat{\alpha}}^{\text{Tr}, M}$	$C_{\widehat{\Gamma}, \pi/2, \hat{\alpha}}^{\text{P}, M}$	$C_{\widehat{\Gamma}, \pi/2, \hat{\alpha}}^{\text{Tr}, M}$	$C_{\widehat{\Gamma}, \pi/2, \hat{\alpha}}^{\text{P}, M}$	$C_{\widehat{\Gamma}, \pi/2, \hat{\alpha}}^{\text{Tr}, M}$
7	0.32431	0.760099	0.325985	0.654654	0.360532	0.654654	0.4152099	0.686161
26	0.338539	0.829445	0.340267	0.761278	0.373669	0.751615	0.4274757	0.863324
63	0.341122	0.831325	0.342556	0.762901	0.375590	0.751994	0.4286444	0.864595
124	0.341147	0.831335	0.342589	0.762905	0.375603	0.751999	0.4286652	0.864630
215	0.341147	0.831335	0.342589	0.762905	0.375603	0.751999	0.4286652	0.864630

Table 4: $C_{\widehat{\Gamma}, \pi/2, \hat{\alpha}}^{\text{P}, M}$ and $C_{\widehat{\Gamma}, \pi/2, \hat{\alpha}}^{\text{Tr}, M}$ with respect to $M(N)$ for $\widehat{T}_{\hat{\theta}, \hat{\alpha}}$ with $\rho = 1$, $\hat{\theta} = \frac{\pi}{2}$, and several $\hat{\alpha}$.

$$\begin{aligned} \|v\|_T &\leq \widetilde{C}_{\Gamma}^{\text{P}} h_1 h_3 \|\nabla v\|_T, \quad \widetilde{C}_{\Gamma}^{\text{P}} = \min_{\hat{\alpha}=\{\pi/4, \pi/3, \pi/2, 2\pi/3\}} \left\{ c_{\pi/2, \hat{\alpha}}^{\text{P}} C_{\widehat{\Gamma}, \pi/2, \hat{\alpha}}^{\text{P}} \right\}, \\ \|v\|_{\Gamma} &\leq \widetilde{C}_{\Gamma}^{\text{Tr}} (h_1 h_3)^{\frac{1}{2}} \|\nabla v\|_T, \quad \widetilde{C}_{\Gamma}^{\text{Tr}} = \min_{\hat{\alpha}=\{\pi/4, \pi/3, \pi/2, 2\pi/3\}} \left\{ c_{\pi/2, \hat{\alpha}}^{\text{Tr}} C_{\widehat{\Gamma}, \pi/2, \hat{\alpha}}^{\text{Tr}} \right\}, \end{aligned} \quad (20)$$

where $C_{\widehat{\Gamma}, \pi/2, \hat{\alpha}}^{\text{P}}$ and $C_{\widehat{\Gamma}, \pi/2, \hat{\alpha}}^{\text{Tr}}$ are the constants related to four reference tetrahedron from Table 4 and $c_{\pi/2, \hat{\alpha}}^{\text{P}}$ and $c_{\pi/2, \hat{\alpha}}^{\text{Tr}}$ are the ratios of the mapping $\mathcal{F}_{\pi/2, \hat{\alpha}}: \widehat{T}_{\pi/2, \hat{\alpha}} \rightarrow T$. Here, $\widehat{T}_{\pi/2, \hat{\alpha}} := \text{conv}\left\{(0, 0, 0), (1, 0, 0), (0, 0, 1), (\cos \hat{\alpha}, \sin \hat{\alpha}, 0)\right\}$ with $\hat{\alpha} = \left\{\frac{\pi}{4}, \frac{\pi}{3}, \frac{\pi}{2}, \frac{2\pi}{3}\right\}$, T is defined in (19), and $\mathcal{F}_{\pi/2, \hat{\alpha}}(\hat{x})$ is presented by the relation

$$x = \mathcal{F}_{\pi/2, \hat{\alpha}}(\hat{x}) = B_{\pi/2, \hat{\alpha}} \hat{x}, \quad B_{\pi/2, \hat{\alpha}} = \begin{pmatrix} h_1 & \frac{h_1}{\sin \hat{\alpha}} (\rho \cos \alpha \sin \theta - \cos \hat{\alpha}) & 0 \\ 0 & h_1 \rho \frac{\sin \alpha \sin(\theta)}{\sin \hat{\alpha}} & 0 \\ 0 & h_1 \rho \frac{\cos \theta}{\sin \hat{\alpha}} & h_3 \end{pmatrix}. \quad (21)$$

Latter mapping ratios depend on the maximum eigenvalue of the matrix

$$\begin{aligned} A_{\pi/2, \hat{\alpha}} &:= \begin{pmatrix} h_1^2 + b_{12}^2 & b_{12}b_{22} & b_{12}b_{32} \\ b_{12}b_{22} & b_{22}^2 & b_{22}b_{32} \\ b_{12}b_{32} & b_{22}b_{32} & h_3^2 + b_{32}^2 \end{pmatrix} \\ &= h_1^2 \cdot \begin{pmatrix} 1 + \frac{1}{\sin^2 \hat{\alpha}} (\rho \cos \alpha \sin \theta - \cos \hat{\alpha})^2 & \frac{\rho \sin \alpha \sin \theta}{\sin^2 \hat{\alpha}} (\rho \cos \alpha \sin \theta - \cos \hat{\alpha}) & \frac{\rho \cos \theta}{\sin^2 \hat{\alpha}} (\rho \cos \alpha \sin \theta - \cos \hat{\alpha}) \\ \frac{\rho \sin \alpha \sin \theta}{\sin^2 \hat{\alpha}} (\rho \cos \alpha \sin \theta - \cos \hat{\alpha}) & \frac{\rho^2 \sin^2 \alpha \cos^2 \theta}{\sin^2 \hat{\alpha}} & \frac{\rho^2 \sin \alpha \sin 2\theta}{2 \sin^2 \hat{\alpha}} \\ \frac{\rho \cos \theta}{\sin^2 \hat{\alpha}} (\rho \cos \alpha \sin \theta - \cos \hat{\alpha}) & \frac{\rho^2 \sin \alpha \sin 2\theta}{2 \sin^2 \hat{\alpha}} & \frac{h_3^2}{h_1^2} + \rho^2 \frac{\cos^2 \theta}{\sin^2 \hat{\alpha}} \end{pmatrix}, \end{aligned}$$

where b_{12}, b_{22}, b_{32} are elements of $\bar{B}_{\pi/2, \hat{\alpha}}$ in (21). Accordingly, $\lambda_{\max}(A_{\pi/2, \hat{\alpha}})$ is defined by the relation

$$\lambda_{\max}(A_{\pi/2, \hat{\alpha}}) = \mu_{\pi/2, \hat{\alpha}} = \mathcal{E}_4^{1/3} - \mathcal{E}_2 \mathcal{E}_4^{-1/3} + \frac{1}{2} \mathcal{E}_1,$$

where

$$\begin{aligned} \mathcal{E}_1 &= b_{12}^2 + b_{22}^2 + b_{32}^2 + h_1^2 + h_3^2, \\ \mathcal{E}_2 &= \frac{1}{3} \left(h_3^2 (b_{12}^2 + b_{22}^2) + h_1^2 (b_{22}^2 + b_{32}^2) - \frac{1}{3} \mathcal{E}_1^2 + h_1^2 h_3^2 \right), \\ \mathcal{E}_3 &= \frac{1}{27} \mathcal{E}_1^3 - \frac{1}{6} \mathcal{E}_1 \left(h_3^2 (b_{12}^2 + b_{22}^2) + h_1^2 (b_{22}^2 + b_{32}^2) + h_1^2 h_3^2 \right) + \frac{1}{2} b_{22}^2 h_1^2 h_3^2, \\ \mathcal{E}_4 &= \mathcal{E}_3 + \left(\left(\frac{h_3^2}{3} (b_{12}^2 + b_{22}^2) + \frac{h_1^2}{3} (b_{22}^2 + b_{32}^2) - \frac{1}{9} \mathcal{E}_1^2 + \frac{1}{3} h_1^2 h_3^2 \right)^3 + \mathcal{E}_3^2 \right)^{1/2}. \end{aligned}$$

Therefore, $c_{\pi/2, \hat{\alpha}}^{\text{P}}$ and $c_{\pi/2, \hat{\alpha}}^{\text{Tr}}$ in (20) reads as follows

$$c_{\pi/2, \hat{\alpha}}^{\text{P}} = \frac{\mu_{\pi/2, \hat{\alpha}}^{1/2}}{h_1 h_3}, \quad c_{\pi/2, \hat{\alpha}}^{\text{Tr}} = \left(\frac{h_3 \sin \hat{\alpha}}{\rho \sin \alpha \sin \theta} \right)^{1/2} c_{\pi/2, \hat{\alpha}}^{\text{P}}.$$

Lower bounds of the constants C_{Γ}^{P} and C_{Γ}^{Tr} are computed by minimization of $\mathcal{R}_{\Gamma}^{\text{P}}[w]$ and $\mathcal{R}_{\Gamma}^{\text{Tr}}[w]$ over the set $V_3^N \subset H^1(T)$, where

$$V_3^N := \left\{ \varphi_{ijk} = x^i y^j z^k, \quad i, j, k = 0, \dots, N, \quad i = j = k \neq 0 \right\}, \quad \dim V_3^N = M(N) := (N+1)^3 - 1.$$

The respective results are presented in Tables 5 and 6 for T with $h_1 = 1, h_3 = 1$, and $\rho = 1$. We note that exact values of constants are probably closer to the numbers presented in left hand side columns. For a fixed angle θ , we also present the data graphically. Fig 10 illustrates estimates of $\underline{C}_{\Gamma}^{M, \text{P}}$ and $\underline{C}_{\Gamma}^{M, \text{Tr}}$ for $\theta = \pi/2$.

	$\alpha = \frac{\pi}{6}$		$\alpha = \frac{\pi}{4}$		$\alpha = \frac{\pi}{3}$		$\alpha = \frac{\pi}{2}$	
θ	$\underline{C}_{\Gamma}^{M, \text{P}}$	$\tilde{C}_{\Gamma}^{\text{P}}$	$\underline{C}_{\Gamma}^{M, \text{P}}$	$\tilde{C}_{\Gamma}^{\text{P}}$	$\underline{C}_{\Gamma}^{M, \text{P}}$	$\tilde{C}_{\Gamma}^{\text{P}}$	$\underline{C}_{\Gamma}^{M, \text{P}}$	$\tilde{C}_{\Gamma}^{\text{P}}$
$\pi/6$	0.23883	0.49035	0.24621	0.49841	0.25870	0.51054	0.29484	0.51308
$\pi/4$	0.23883	0.45388	0.24621	0.46173	0.25870	0.47683	0.29484	0.49075
$\pi/3$	0.29666	0.41958	0.31194	0.42259	0.33489	0.43724	0.38976	0.46002
$\pi/2$	0.34302	0.35667	0.34112	0.34115	0.34256	0.34259	0.37559	0.37560
$2\pi/3$	0.40428	0.41958	0.40562	0.42259	0.40927	0.43724	0.42867	0.46002
$3\pi/4$	0.42890	0.45388	0.43110	0.46173	0.43505	0.47683	0.45017	0.49075
$5\pi/6$	0.44964	0.49035	0.45193	0.49841	0.45539	0.51054	0.46607	0.51308
	$\alpha = \frac{\pi}{2}$		$\alpha = \frac{2\pi}{3}$		$\alpha = \frac{3\pi}{4}$		$\alpha = \frac{5\pi}{6}$	
θ	$\underline{C}_{\Gamma}^{M, \text{P}}$	$\tilde{C}_{\Gamma}^{\text{P}}$	$\underline{C}_{\Gamma}^{M, \text{P}}$	$\tilde{C}_{\Gamma}^{\text{P}}$	$\underline{C}_{\Gamma}^{M, \text{P}}$	$\tilde{C}_{\Gamma}^{\text{P}}$	$\underline{C}_{\Gamma}^{M, \text{P}}$	$\tilde{C}_{\Gamma}^{\text{P}}$
$\pi/6$	0.29484	0.51308	0.33069	0.51792	0.34468	0.52253	0.35499	0.52694
$\pi/4$	0.29484	0.49075	0.33069	0.50261	0.34468	0.51308	0.35499	0.52253
$\pi/3$	0.38976	0.46002	0.43880	0.48413	0.45742	0.50261	0.47106	0.51792
$\pi/2$	0.37559	0.37560	0.42865	0.42867	0.45017	0.45731	0.46607	0.47811
$2\pi/3$	0.42867	0.46002	0.45997	0.48413	0.47457	0.50261	0.48598	0.51792
$3\pi/4$	0.45017	0.49075	0.47204	0.50261	0.48239	0.51308	0.49064	0.52253
$5\pi/6$	0.46607	0.51308	0.47972	0.51792	0.48607	0.52253	0.49115	0.52694

Table 5: $\underline{C}_{\Gamma}^{M, \text{P}}(M(N) = 124)$ and $\tilde{C}_{\Gamma}^{\text{P}}$.

5 Example

Constants in the Friedrichs', Poincaré, and other functional inequalities arise in various problems of numerical analysis and often we need to know values of the respective constants associated with particular domains. Results related to constants in extension estimates and projection type estimates related to finite element approximations can be found in, e.g., [11, 4] and in many other publications. Concerning constants in the trace inequalities associated with polygonal domain, we mention the paper [2]. Constants in functional (embedding) inequalities arise in a posteriori estimates of the functional type (see [17] and the references therein). Below we pay attention to the latter case and first in general terms explain reasons that invoke the constants.

Let u denote the exact solution of an elliptic boundary value problem generated by the pair of conjugate operators grad and $-\text{div}$ (e.g., the problem (25)–(28) considered below) and v be a function in the energy space satisfying

	$\alpha = \frac{\pi}{6}$		$\alpha = \frac{\pi}{4}$		$\alpha = \frac{\pi}{3}$		$\alpha = \frac{\pi}{2}$	
θ	$\underline{C}_\Gamma^{M,\text{Tr}}$	$\tilde{C}_\Gamma^{\text{Tr}}$	$\underline{C}_\Gamma^{M,\text{Tr}}$	$\tilde{C}_\Gamma^{\text{Tr}}$	$\underline{C}_\Gamma^{M,\text{Tr}}$	$\tilde{C}_\Gamma^{\text{Tr}}$	$\underline{C}_\Gamma^{M,\text{Tr}}$	$\tilde{C}_\Gamma^{\text{Tr}}$
$\pi/6$	1.09760	3.78259	0.96245	2.71866	0.91255	2.27382	0.93123	2.05449
$\pi/4$	1.09760	2.43897	0.96245	1.78094	0.91255	1.50166	0.93123	1.38951
$\pi/3$	0.89122	1.74467	0.79146	1.31130	0.75950	1.12431	0.78904	1.06349
$\pi/2$	0.98017	1.22920	0.83132	0.83133	0.76290	0.76291	0.75199	0.75200
$2\pi/3$	1.17698	1.74467	0.99473	1.31130	0.90578	1.12431	0.86463	1.06349
$3\pi/4$	1.35195	2.43897	1.14144	1.78094	1.03737	1.50166	0.98220	1.38951
$5\pi/6$	1.65317	3.78259	1.39424	2.71866	1.26490	2.27382	1.19017	2.05449
	$\alpha = \frac{\pi}{2}$		$\alpha = \frac{2\pi}{3}$		$\alpha = \frac{3\pi}{4}$		$\alpha = \frac{5\pi}{6}$	
θ	$\underline{C}_\Gamma^{M,\text{Tr}}$	$\tilde{C}_\Gamma^{\text{Tr}}$	$\underline{C}_\Gamma^{M,\text{Tr}}$	$\tilde{C}_\Gamma^{\text{Tr}}$	$\underline{C}_\Gamma^{M,\text{Tr}}$	$\tilde{C}_\Gamma^{\text{Tr}}$	$\underline{C}_\Gamma^{M,\text{Tr}}$	$\tilde{C}_\Gamma^{\text{Tr}}$
$\pi/6$	0.93123	2.05449	1.07244	2.39471	1.21573	2.95902	1.47044	4.21999
$\pi/4$	0.93123	1.38951	1.07244	1.64324	1.21573	2.01841	1.47044	2.80588
$\pi/3$	0.78904	1.06349	0.91773	1.27423	1.04309	1.50833	1.26357	2.11790
$\pi/2$	0.75199	0.75200	0.86459	0.86463	0.98220	1.12971	1.19017	1.67033
$2\pi/3$	0.86463	1.06349	0.96174	1.27423	1.08134	1.50833	1.30191	2.11790
$3\pi/4$	0.98220	1.38951	1.07921	1.64324	1.20686	2.01841	1.44721	2.80588
$5\pi/6$	1.19017	2.05449	1.29582	2.39471	1.44268	2.95902	1.72383	4.21999

Table 6: $\underline{C}_\Gamma^{M,\text{Tr}}$ ($M(N) = 124$) and $\tilde{C}_\Gamma^{\text{Tr}}$.

the prescribed (Dirichlét) boundary conditions. Typically, the error $e := u - v$ is measured in terms of the energy norm $\|\nabla e\|$ (or some other equivalent norm), which square is bounded from above by the quantities

$$\int_{\Omega} R(v, \text{div}q) e \, dx, \quad \int_{\Omega} D(\nabla v, q) \cdot \nabla e \, dx, \quad \text{and} \quad \int_{\Gamma_N} R_{\Gamma_N}(v, q \cdot n) e \, ds,$$

where Γ_N is the Neumann part of the boundary $\partial\Omega$, n is the outward unit normal, and q is an approximation of the dual variable (flux). The terms R , D , and R_{Γ_N} represent residuals of the differential (balance) equation, constitutive (duality) relation, and Neumann boundary condition, respectively. Since v and q are known from a numerical solution, fully computable estimates are obtained if these integrals are estimated by the Hölder, Friedrichs, and trace inequalities, which involve the corresponding constants. However, a Lipschitz domain Ω with piecewise smooth (e.g., polynomial) boundaries these constants may be difficult to find. A way to avoid these difficulties is suggested by modifications of the estimates using ideas of domain decomposition. Assume that Ω is polygonal (polyhedral) domain decomposed into a collection of non-overlapping convex polygonal sub-domains Ω_i , i.e.,

$$\bar{\Omega} := \bigcup_{\Omega_i \subset \mathcal{O}_\Omega} \bar{\Omega}_i, \quad \mathcal{O}_\Omega := \left\{ \Omega_i \subset \Omega \mid \Omega_{i'} \cap \Omega_{i''} = \emptyset, \, i' \neq i'', \, i = 1, \dots, N \right\}.$$

We denote the set of all edges (faces) by \mathcal{G} and the set of all interior edges by \mathcal{G}_{int} (i.e, $\Gamma_{ij} \subset \mathcal{G}_{\text{int}}$, if $\Gamma_{ij} = \bar{\Omega}_i \cap \bar{\Omega}_j$). Analogously, \mathcal{G}_N denotes the set of edges on Γ_N . The latter set is decomposed into $\Gamma_{N_k} := \Gamma_N \cap \partial\Omega_k$, size $\Gamma_{N_k} = K_N$. Now, the integrals associated with R and R_{Γ_N} can be replaced by sums of local quantities

$$\sum_{i=1}^N \int_{\Omega_i} R_\Omega(v, \text{div}q) e \, dx, \quad \text{and} \quad \sum_{k=1}^{K_N} \int_{\Gamma_{N_k}} R_{\Gamma_N}(v, q \cdot n) e \, ds.$$

If the residuals satisfy the conditions

$$\int_{\Omega_i} R_\Omega(v, \text{div}q) \, dx = 0, \quad \forall i = 1, \dots, N,$$

and

$$\int_{\Gamma_{N_k}} R_{\Gamma_N}(v, q \cdot n) \, ds = 0, \quad \forall k = 1, \dots, K_N,$$

then

$$\int_{\Omega_i} R_\Omega(v, \text{div}q) e \, dx \leq C_{\Omega_i}^P \|R_\Omega(v, \text{div}q)\|_{\Omega_i} \|\nabla e\|_{\Omega_i}, \quad (22)$$

and

$$\int_{\Gamma_{N_k}} R_{\Gamma_N}(v, q \cdot n) e \, ds \leq C_{\Gamma_N}^{\text{Tr}} \|R_{\Gamma_N}(v, q \cdot n)\|_{\Gamma_{N_k}} \|\nabla e\|_{\Omega_k}. \quad (23)$$

Hence, we can deduce a computable upper bound of the error that contains local constants $C_{\Omega_i}^{\text{P}}$ and $C_{\Gamma_{N_k}}^{\text{Tr}}$ for simple subdomains (e.g., triangles or tetrahedrons) instead of the global constants associated with Ω .

The constant C_{Ω}^{P} may arise if, e.g., nonconforming approximations are used. For example, if v does not exactly satisfy the Dirichlet boundary condition on Γ_D , then in the process of estimation it may be necessary to evaluate terms of the type

$$\int_{\Gamma_{D_k}} G_D(v) e \, ds, \quad k = 1, \dots, K_D,$$

where Γ_{D_k} is a part of Γ_D associated with a certain Ω_k , and $G_D(v)$ is a residual generated by inexact satisfaction of the boundary condition. If we impose the requirement that the Dirichlet boundary condition is satisfied in a weak sense, i.e., $\{G_D(v)\}_{\Gamma_{D_k}} = 0$, then each boundary integral can be estimated as follows:

$$\int_{\Gamma_{D_k}} G_D(v) e \, ds \leq C_{\Gamma_{D_k}}^{\text{P}} \|G_D(v)\|_{\Gamma_{D_k}} \|\nabla e\|_{\Omega_k}. \quad (24)$$

After summing (22), (23), and (24), we obtain a product of weighted norms of localized residuals (which are known) and $\|\nabla e\|_{\Omega}$. Since the sum is bounded from below by the squared energy norm, we arrive at computable error majorant.

Now, we discuss these questions in more detail with the paradigm of the following boundary value problem: find u such that

$$-\operatorname{div} p + \varrho^2 u = f, \quad \text{in } \Omega, \quad (25)$$

$$p = A \nabla u, \quad \text{in } \Omega, \quad (26)$$

$$u = u_D, \quad \text{on } \Gamma_D, \quad (27)$$

$$A \nabla u \cdot n = F \quad \text{on } \Gamma_N. \quad (28)$$

Here $f \in L^2(\Omega)$, $F \in L^2(\Gamma_N)$, $u_D \in H^1(\Omega)$, and A is a symmetric positive definite matrix with bounded coefficients satisfying the condition $\lambda_1 |\xi|^2 \leq A \xi \cdot \xi$, where λ_1 is a positive constant independent of ξ . The generalized solution of (25)–(28) exists and is unique in the set $V_0 + u_D$, where $V_0 := \{w \in H^1(\Omega) \mid w = 0 \text{ on } \Gamma_D\}$.

Assume that $v \in V_0 + u_D$ is a conforming approximation of u . We wish to find a computable majorant of the error norm

$$\|e\| := \|\nabla e\|_A^2 + \|\varrho e\|^2, \quad (29)$$

where $\|\nabla e\|_A^2 := \int_{\Omega} A \nabla e \cdot \nabla e \, dx$. First, we note that the integral identity that defines u can be rewritten in the form

$$\int_{\Omega} A \nabla e \cdot \nabla w \, dx + \int_{\Omega} \varrho^2 e w \, dx = \int_{\Omega} (f w - \varrho^2 v w - A \nabla v \cdot \nabla w) \, dx + \int_{\Gamma_N} F w \, ds, \quad \forall w \in V_0. \quad (30)$$

It is well known (see [17, Section 4.2]) that this relation yields computable majorant of $\|\nabla e\|_A$, if we introduce a vector valued function $q \in H(\Omega, \operatorname{div})$ and transform (30) by means of integration by parts relations. The majorant has the form

$$\|e\| \leq \|D_{\Omega}(\nabla v, q)\|_{A^{-1}} + C_1 \|R(v, \operatorname{div} q)\|_{\Omega} + C_2 \|R_{\Gamma_N}(v, q \cdot n)\|_{\Gamma_N}, \quad (31)$$

where C_1 and C_2 are positive constants explicitly defined by λ_1 , C^{F} is the constant in the Friedrichs' inequality $\|v\|_{\Omega} \leq C^{\text{F}} \|\nabla v\|_{\Omega}$ for functions vanishing on Γ_D , and $C_{\Gamma_N}^{\text{Tr}}$ is the constant in the trace inequality associated with Γ_N . The integrands are defined by the relations

$$D(\nabla v, q) := A \nabla v - q, \quad R(v, \operatorname{div} q) := \operatorname{div} q + f - \varrho^2 v, \quad \text{and} \quad R_{\Gamma_N}(v, q \cdot n) := q \cdot n - F.$$

In general, finding C^{F} and $C_{\Gamma_N}^{\text{Tr}}$ may be not an easy task. We can exclude C_2 if q additionally satisfies the condition $q \cdot n = F$. Then, the last term in (31) vanishes. However, this condition is difficult to satisfy if F is a complicated nonlinear function. In order to exclude C_1 , we can apply domain decomposition and use (22) instead of the global estimate. Then, the estimate will operate with the constants $C_{\Omega_i}^{\text{P}}$ (which upper bounds are known for convex

domains). Moreover, it is shown below that using the inequalities (2) and (4), we can essentially weaken the assumptions required for the variable q .

Define the space of vector valued functions

$$\hat{H}(\Omega, \mathcal{O}_\Omega, \text{div}) := \left\{ q \in L^2(\Omega, \mathbb{R}^d) \mid q = q_i \in H(\Omega_i, \text{div}), \quad \{\{\text{div}q_i + f - \varrho^2 v\}\}_{\Omega_i} = 0, \quad \forall \Omega_i \subset \mathcal{O}_\Omega, \right. \\ \left. \{\{(q_i - q_j) \cdot n_{ij}\}\}_{\Gamma_{ij}} = 0, \quad \forall \Gamma_{ij} \subset \mathcal{G}_{\text{int}}, \quad \{\{q_i \cdot n_k - F\}\}_{\Gamma_{N_k}} \text{ ds} = 0, \quad \forall k = 1, \dots, K_N \right\}.$$

We note that the space $\hat{H}(\Omega, \mathcal{O}_\Omega, \text{div})$ is wider than $H(\Omega, \text{div})$ (so that we have more flexibility in finding optimal reconstruction of numerical fluxes). Indeed, the vector valued functions in $H(\Omega, \text{div})$ must have continuous normal components on all Γ_{ij} and satisfy the Neumann boundary condition in the pointwise sense. The functions in $\hat{H}(\Omega, \mathcal{O}_\Omega, \text{div})$ satisfy much weaker conditions: namely, the normal components are continuous only in terms of mean values (integrals) and the Neumann condition must hold in the integral sense only.

We reform (30) by means of the integral identity

$$\sum_{\Omega_i \subset \mathcal{O}_\Omega} \int_{\Omega_i} (q \cdot \nabla w + \text{div}q w) \, dx = \sum_{\Gamma_{ij} \subset \mathcal{G}_{\text{int}}} \int_{\Gamma_{ij}} (q_i - q_j) \cdot n_{ij} w \, ds + \sum_{\Gamma_{N_k} \subset \Gamma_N} \int_{\Gamma_{N_k}} (q_i \cdot n_i - F) w \, ds,$$

which holds for any $w \in V_0$ and $q \in \hat{H}(\Omega, \mathcal{O}_\Omega, \text{div})$. Setting $w = e$ in (30) and applying the Hölder inequality, we find that

$$\|e\|^2 \leq \|D(\nabla v, q)\|_{A^{-1}} \|\nabla e\|_A + \sum_{\Omega_i \subset \mathcal{O}_\Omega} \|R(v, \text{div}q)\|_{\Omega_i} \|e - \{e\}_{\Omega_i}\|_{\Omega_i} \\ + \sum_{\Gamma_{ij} \subset \mathcal{G}_{\text{int}}} r_{ij}(q) \|e - \{e\}_{\Gamma_{ij}}\|_{\Gamma_{ij}} + \sum_{\Gamma_{N_k} \subset \Gamma_N} \rho_k(q) \|e - \{e\}_{\Gamma_{N_k}}\|_{\Gamma_{N_k}},$$

where

$$r_{ij}(q) := \|(q_i - q_j) \cdot n_{ij}\|_{\Gamma_{ij}}, \quad \rho_k(q) := \|q_i \cdot n_i - F\|_{\Gamma_{N_k}}.$$

In view of (1) and (4), we obtain

$$\|e\|^2 \leq \|D(\nabla v, q)\|_{A^{-1}} \|\nabla e\|_A + \sum_{\Omega_i \subset \mathcal{O}_\Omega} \|R(v, \text{div}q)\|_{\Omega_i} C_{\Omega_i}^{\text{P}} \|\nabla e\|_{\Omega_i} \\ + \sum_{\Gamma_{ij} \subset \mathcal{G}_{\text{int}}} r_{ij}(q) C_{\Gamma_{ij}}^{\text{Tr}} \|\nabla e\|_{\Omega_i} + \sum_{\Gamma_{N_k} \subset \Gamma_N} \rho_k(q) C_{\Gamma_{N_k}}^{\text{Tr}} \|\nabla e\|_{\Omega_i}. \quad (32)$$

The second term in the right hand side is estimated by the quantity $\mathfrak{R}_1(v, q) \|\nabla e\|_\Omega$, where

$$\mathfrak{R}_1^2(v, q) := \sum_{\Omega_i \subset \mathcal{O}_\Omega} \frac{(\text{diam } \Omega_i)^2}{\pi^2} \|R(v, \text{div}q)\|_{\Omega_i}^2.$$

We can represent any $\Omega_i \subset \mathcal{O}_\Omega$ as a sum of simplexes such that each simplex has one edge on $\partial\Omega_i$. Let $C_{i, \max}^{\text{Tr}}$ denote the largest constant in the respective Poincaré type inequalities (4) associated with all edges of $\partial\Omega_i$. Then, the last two terms of (32) can be estimated by the quantity $\mathfrak{R}_2(v, q) \|\nabla e\|_\Omega$, where

$$\mathfrak{R}_2^2(q) := \sum_{\Omega_i \subset \mathcal{O}_\Omega} (C_{i, \max}^{\text{Tr}})^2 \eta_i^2,$$

and

$$\eta_i^2 = \sum_{\substack{\Gamma_{ij} \subset \mathcal{G}_{\text{int}} \\ \Gamma_{ij} \cap \partial\Omega_i \neq \emptyset}} \frac{1}{4} r_{ij}^2(q) + \sum_{\substack{\Gamma_k \subset \mathcal{G}_N \\ \Gamma_k \cap \partial\Omega_i \neq \emptyset}} \rho_k^2(q).$$

Then, (32) yields the estimate

$$\|e\|^2 \leq \|D(\nabla v, q)\|_{A^{-1}} \|\nabla e\|_A + (\mathfrak{R}_1(v, q) + \mathfrak{R}_2(q)) \|\nabla e\|_\Omega,$$

which shows that

$$\|e\| \leq \|D(\nabla v, q)\|_{A^{-1}} + \frac{1}{\lambda_1} \left(\mathfrak{R}_1(v, q) + \mathfrak{R}_2(q) \right). \quad (33)$$

Here, the term $\mathfrak{R}_2(q)$ controls violations of conformity of q (on interior edges) and inexact satisfaction of boundary conditions (on edges related to Γ_N). It is easy to see that $\mathfrak{R}_2(q) = 0$, if and only if $q \cdot n$ is continuous on \mathcal{G}_{int} and exactly satisfy the boundary condition. Hence, it can be viewed as a measure of the “flux nonconformity”. Other terms have the same meaning as in known a posteriori estimates of the functional type, namely, the first term measures the violation in the relation $q = A\nabla v$ (cf. (26)), and $\mathfrak{R}_1(v, q)$ measures inaccuracy in the equilibrium (balance) equation (25). The right-hand side of (33) contains known functions (approximation v and the reconstruction of the flux q) and constants that can be easily computed using results of Section 2-4. Finally, we note that estimates similar to (33) were derived in [18] for elliptic variational inequalities and in [9] for a class of parabolic problems.

References

- [1] R. Bañuelos and K. Burdzy. On the “hot spots” conjecture of J. Rauch. *J. Funct. Anal.*, 164(1):1–33, 1999.
- [2] C. Carstensen and S. A. Sauter. A posteriori error analysis for elliptic PDEs on domains with complicated structures. *Numer. Math.*, 96(4):691–721, 2004.
- [3] S. Y. Cheng. Eigenvalue comparison theorems and its geometric applications. *Math. Z.*, 143(3):289–297, 1975.
- [4] P. G. Ciarlet. *The finite element method for elliptic problems*. North-Holland Publishing Co., Amsterdam-New York-Oxford, 1978. Studies in Mathematics and its Applications, Vol. 4.
- [5] Clark R. Dohrmann, Axel Klawonn, and Olof B. Widlund. Domain decomposition for less regular subdomains: overlapping Schwarz in two dimensions. *SIAM J. Numer. Anal.*, 46(4):2153–2168, 2008.
- [6] M. Fuchs. Computable upper bounds for the constants in Poincaré-type inequalities for fields of bounded deformation. *Math. Methods Appl. Sci.*, 34(15):1920–1932, 2011.
- [7] Axel Klawonn, Oliver Rheinbach, and Olof B. Widlund. An analysis of a FETI-DP algorithm on irregular subdomains in the plane. *SIAM J. Numer. Anal.*, 46(5):2484–2504, 2008.
- [8] R. S. Laugesen and B. A. Siudeja. Minimizing Neumann fundamental tones of triangles: an optimal Poincaré inequality. *J. Differential Equations*, 249(1):118–135, 2010.
- [9] S. Matculevich, P. Neittaanmäki, and S. Repin. A posteriori error estimates for time-dependent reaction-diffusion problems based on the Payne–Weinberger inequality. *AIMS*, 35(6), 2015.
- [10] B. J. McCartin. Eigenstructure of the equilateral triangle. II. The Neumann problem. *Math. Probl. Eng.*, 8(6):517–539, 2002.
- [11] S. G. Mikhlin. *Constants in some inequalities of analysis*. A Wiley-Interscience Publication. John Wiley and Sons, Ltd., Chichester, 1986. Translated from the Russian by Reinhard Lehmann.
- [12] A. I. Nazarov and S. I. Repin. Exact constants in Poincaré type inequalities for functions with zero mean boundary traces. *Mathematical Methods in the Applied Sciences*, 2014. Published in arXiv.org in 2012, math/1211.2224.
- [13] Dirk Pauly. On Maxwell’s and Poincaré’s constants. *Discrete Contin. Dyn. Syst. Ser. S*, 8(3):607–618, 2015.
- [14] L. E. Payne and H. F. Weinberger. An optimal Poincaré inequality for convex domains. *Arch. Rational Mech. Anal.*, 5:286–292 (1960), 1960.
- [15] H. Poincaré. Sur les Equations aux Derivees Partielles de la Physique Mathematique. *Amer. J. Math.*, 12(3):211–294, 1890.
- [16] H. Poincaré. Sur les Equations de la Physique Mathematique. *Rend. Circ. Mat. Palermo*, 8:57–156, 1894.
- [17] S. Repin. *A posteriori estimates for partial differential equations*, volume 4 of *Radon Series on Computational and Applied Mathematics*. Walter de Gruyter GmbH & Co. KG, Berlin, 2008.
- [18] S. Repin. Estimates of deviations from exact solutions of variational inequalities based upon payne-weinberger inequality. *J. Math. Sci. (N. Y.)*, 157(6):874–884, 2009.
- [19] Andrea Toselli and Olof Widlund. *Domain decomposition methods—algorithms and theory*, volume 34 of *Springer Series in Computational Mathematics*. Springer-Verlag, Berlin, 2005.

6 Appendix

For convenience, we collect in this part the graphics cited in Section 3 and 4.

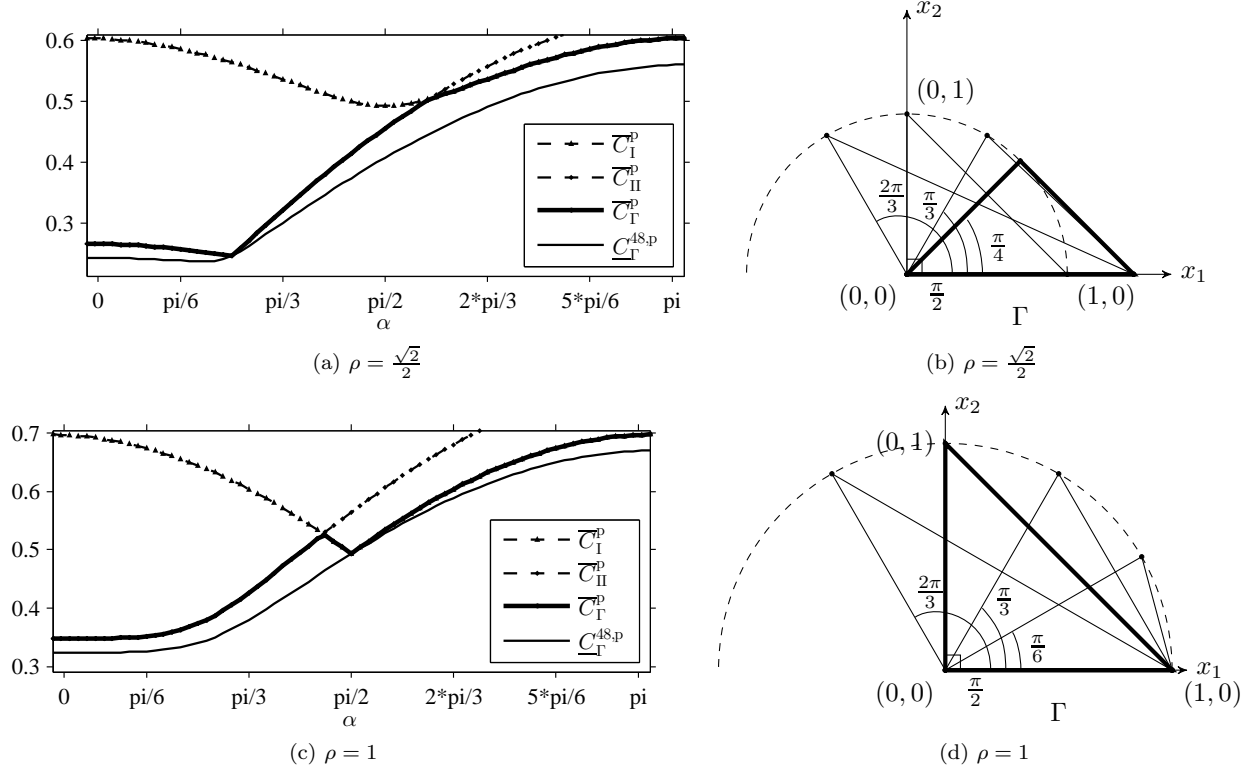


Figure 3: Lower and upper bounds of C_Γ^p for $T \in \mathbb{R}^2$ (a)-(b) $\rho = \frac{\sqrt{2}}{2}$ and (c)-(d) $\rho = 1$.

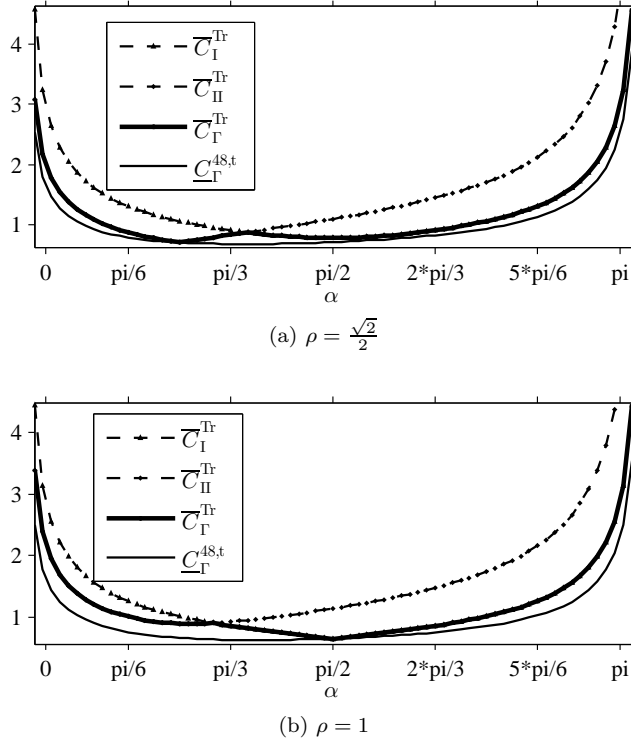
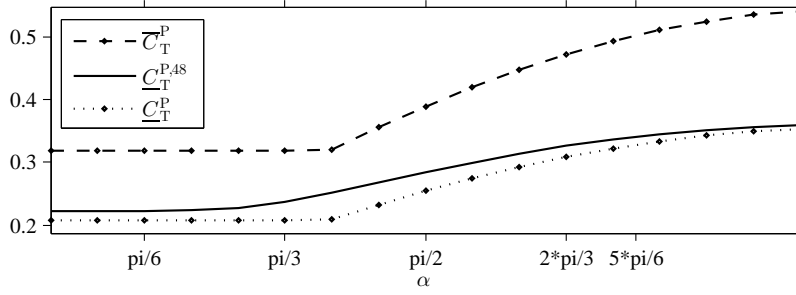
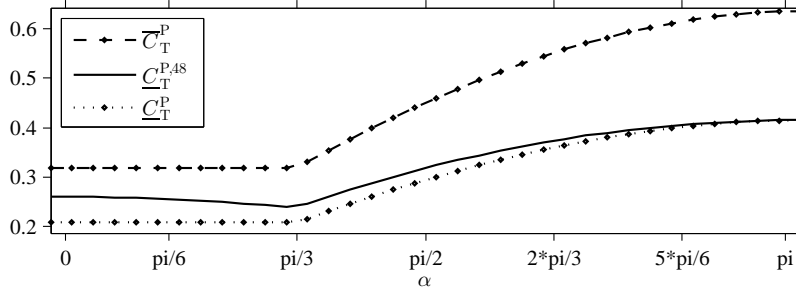


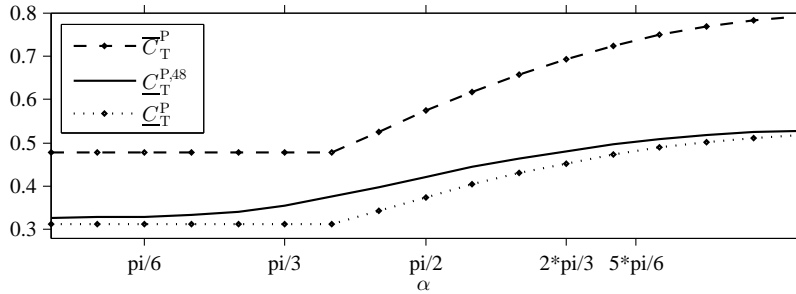
Figure 4: Lower and upper bound of C_Γ^{Tr} for $T \in \mathbb{R}^2$ (a) $\rho = \frac{\sqrt{2}}{2}$ and (b) $\rho = 1$.



(a) $\rho = \frac{\sqrt{2}}{2}$



(b) $\rho = 1$



(c) $\rho = \frac{3}{2}$

Figure 5: \underline{C}_T^{48} with upper and lower bounds with respect to α on T with (a) $\rho = \frac{\sqrt{2}}{2}$ and (b) $\frac{3}{2}$.

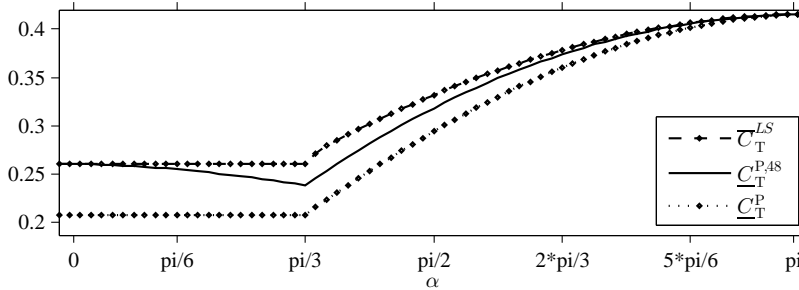


Figure 6: Approximation \underline{C}_T^{48} with improved upper and lower bounds on isosceles T with respect to α .

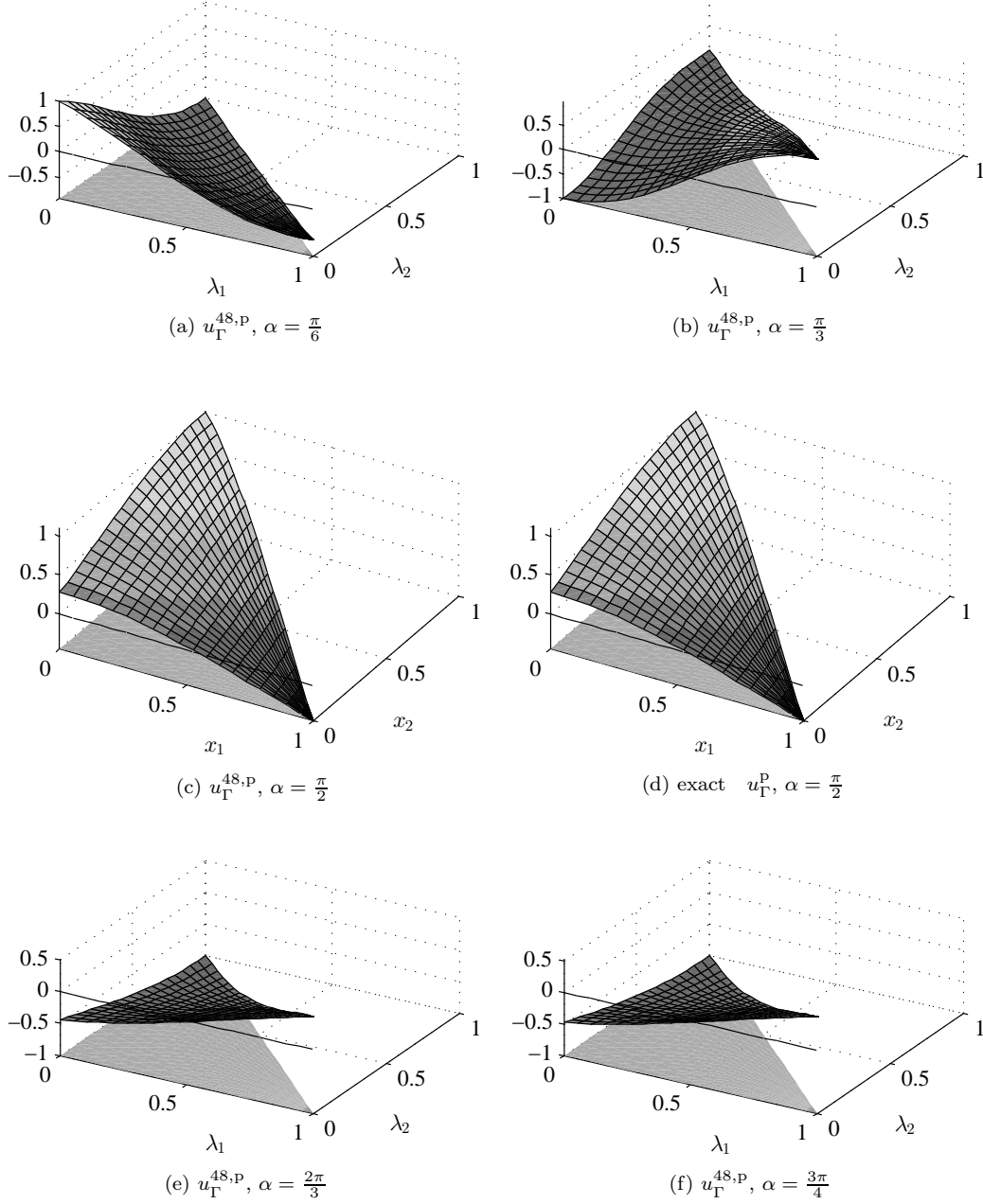


Figure 7: Eigenfunctions corresponding to $\underline{C}_{\Gamma}^{M,P}$ and $\underline{C}_{\Gamma}^{M,Tr}$ for $M = 48$ on simplex T with $\rho = 1$ and different α .

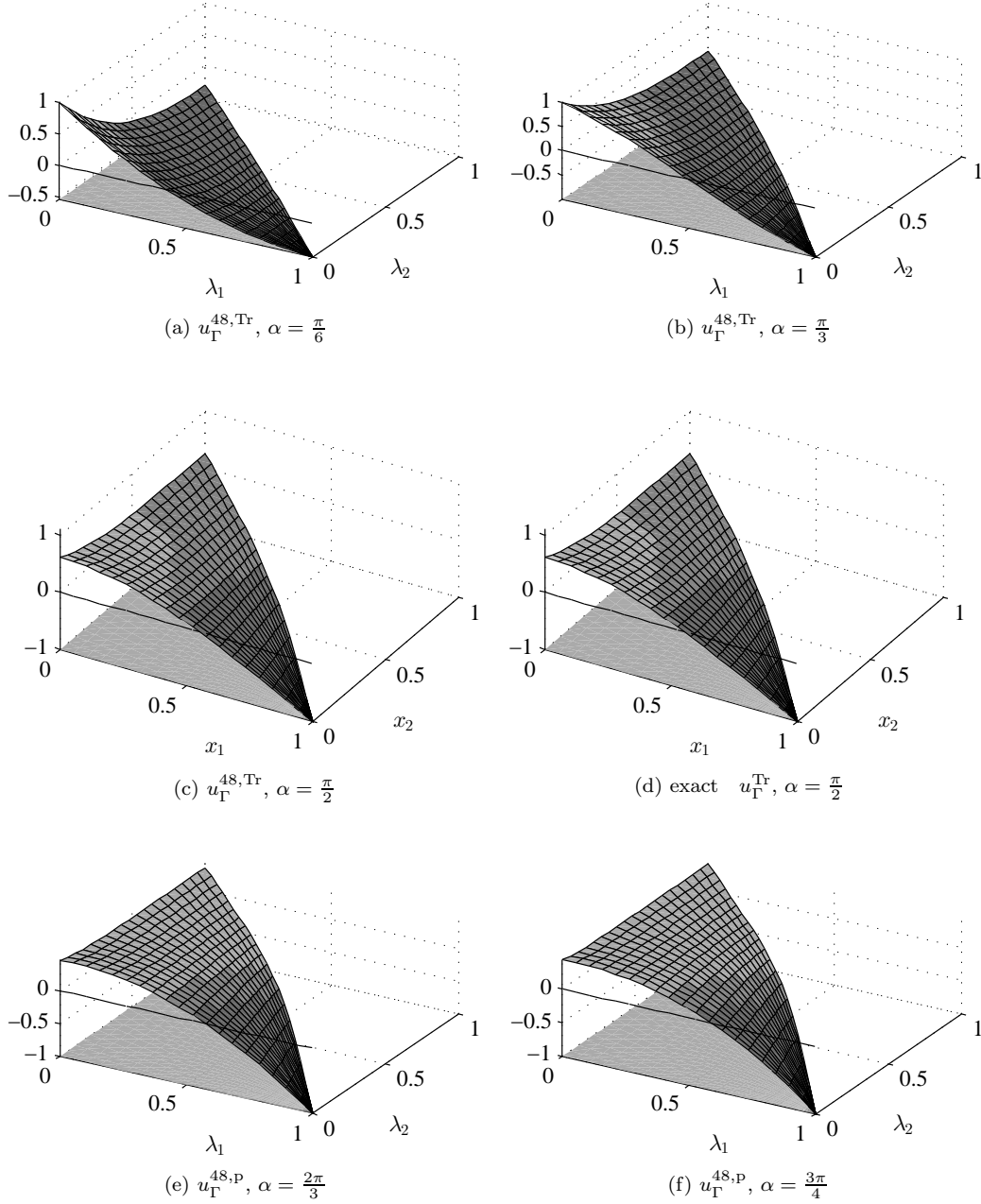


Figure 8: Eigenfunctions corresponding to $\underline{C}_{\Gamma}^{M, \text{P}}$ and $\underline{C}_{\Gamma}^{M, \text{Tr}}$ for $M = 48$ on simplex T with $\rho = 1$ and different α .

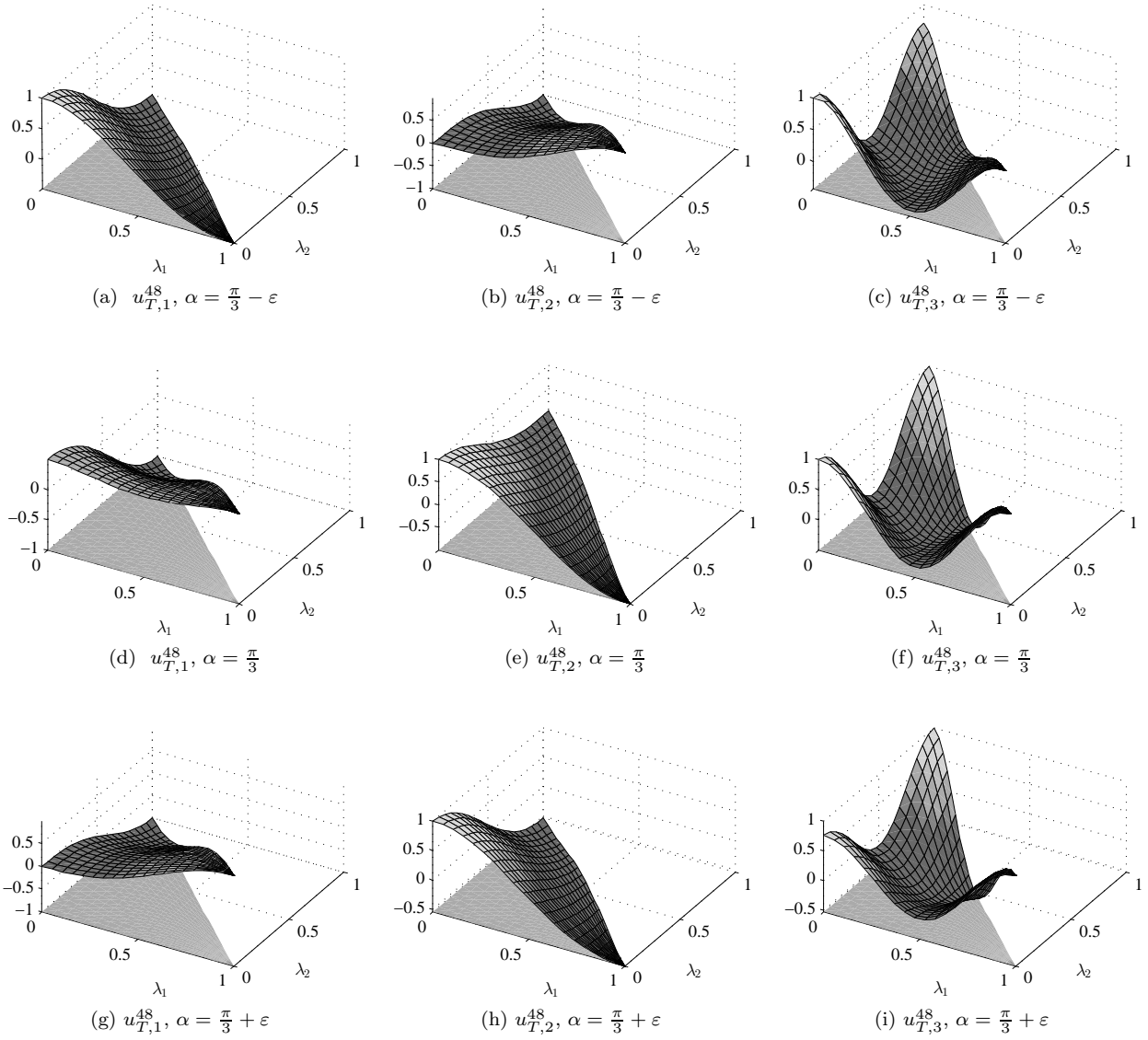


Figure 9: Eigenfunctions corresponding to $\underline{C}_T^{M,P}$ with $M = 48$ on isosceles triangles $T \in \mathbb{R}^2$ with $\alpha = \frac{\pi}{3}, \frac{\pi}{3} - \varepsilon,$ and $\frac{\pi}{3} + \varepsilon$ in barycentric coordinates.

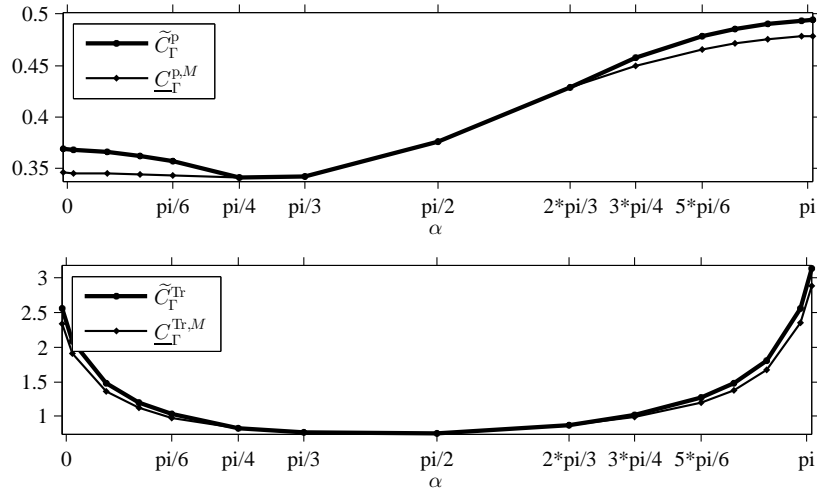


Figure 10: C_T^P and C_T^{Tr} for $T \in \mathbb{R}^3$ with $H = 1, \rho = 1$ with estimate based on four reference tetrahedrons.